Kaersutite-bearing xenoliths and megacrysts in volcanic rocks from the Funk Seamount in the southwest Indian Ocean

ARCH M. REID* AND ANTON P. LE ROEX

Department of Geology, University of Cape Town, Rondebosch 7700, South Africa

Abstract

Eight samples (seven volcanic rocks and one quartz sandstone) have been dredged from the Funk Seamount, 60 km NW of Marion Island in the southwest Indian Ocean (lat. 46° 15′ S, long. 37° 20′ E). The volcanic rocks are fine-grained vesicular basanitoids and glass-rich volcanic breccias geochemically similar to the Marion Island lavas. Lavas and breccias contain a suite of megacryst minerals and of small polymineralic xenoliths, in both of which kaersutite is a prominent constituent.

The megacryst suite comprises large unzoned single grains of kaersutite, plagioclase, pyroxene, magnetite and ilmenite, all showing textural evidence of resorption/reaction with the basanitoid host. The megacrysts have a limited range of compositions except for the plagioclase which ranges from oligoclase to labradorite.

The small (2 mm to ~ 3 cm) xenoliths are mostly two-pyroxene amphibole assemblages with or without olivine, magnetite, ilmenite, plagioclase and apatite. The xenoliths show some evidence of reaction with the basanitoid host and most have undergone recrystallization and/or localised decompression melting.

Xenolith and megacryst assemblages are interpreted as being associated with the formation and partial crystallization of a hydrous basanitoid melt at depth.

KEYWORDS: kaersutite, amphibole, xenolith, Funk Seamount, Indian Ocean.

Introduction

FUNK SEAMOUNT is a prominent seamount situated 60 km to the NW of Marion and Prince Edward Islands. Fig. 1 shows the position of the Funk Seamount relative to the Prince Edward Islands and to the Southwest Indian Ridge. The seamount was named after Ernst Funk, former captain of the S.A. Agulhas.

On May 28 1979 the S.A. Agulhas (cruise 7) was utilized for the first time to dredge ocean bottom samples using the Funk Seamount as a target, at a water depth of 300 m. Eight samples were dredged from the seamount, seven of which are volcanic rocks with chemical and mineralogical similarities to each other, and to the volcanic products of Marion Island. The other sample is a fragment of quartz sandstone. The volcanic samples are vesicular lavas and fragmental feldspar-olivine vitrophyres: both varieties contain small ultramafic xenoliths and a suite of mostly monomineralic megacrysts. Brown amphibole is a prominent constituent of both xenolith and megacryst suites.

Mantle xenoliths in abyssal lavas are rare and so these samples are of particular interest. In this article we report on the petrography, mineral chemistry, and whole rock compositions of the volcanic rocks and on the mineral chemistry of their inclusions. This is followed by a brief discussion on the possible relationships between the volcanic rocks, the megacrysts, and the xenoliths.

* Present address: Department of Geosciences, University of Houston, Houston, Texas 77004, USA.

Mineralogical Magazine, June 1988, Vol. 52, pp. 359–70

Petrography

Sample D1D is an orthoquartzite that is unlikely to be of local derivation and may have been ice-rafted to the vicinity of the Funk Seamount. The other samples all have alkali basalt affinities and carry a distinctive brown amphibole as a megacryst or within xenoliths. These rocks thus appear to be genetically related (a contention supported by bulk rock compositions—see later section) and to have originated from the Funk Seamount.

The four lava samples (D1A2, D1B1, D1B2,

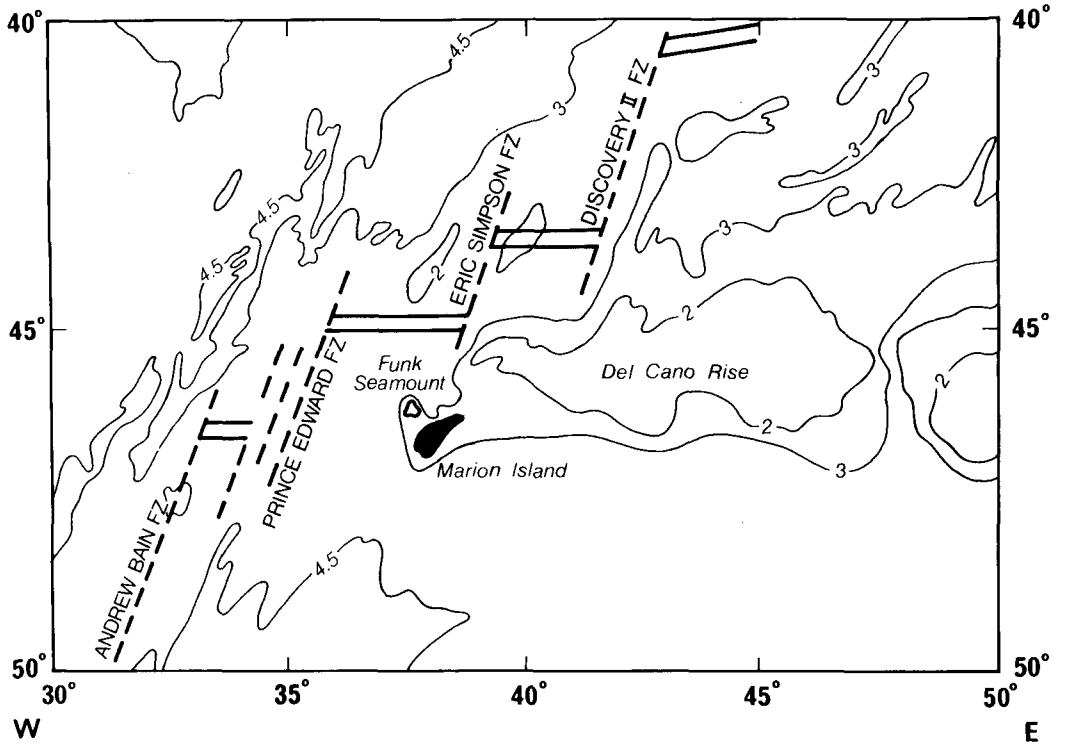

FIG. 1. Sketch map of the Southwest Indian Ocean showing the Southwest Indian Ridge system and the locations of the Funk Seamount and Marion Island.

D1E) are petrographically similar, differing mainly in size and shape of vesicles and the extent to which a flow structure has developed. All are fine grained with abundant feldspar laths, commonly in flow alignment (Fig. 2*a*). Olivine occurs as subhedral to euhedral grains, commonly as microphenocrysts, whereas anhedral clinopyroxene is confined to the matrix which is generally very fine grained with abundant equant opaque oxides.

The glassy lava fragments in the breccias (D1A1, D1C1) are also finely vesicular and comprise microphenocrysts of plagioclase, olivine and less abundant opaque oxides in clear light yellow glass (Fig. 2*b*).

The megacrysts, common in both lavas and breccias, are clinopyroxene, rare orthopyroxene, amphibole (Fig. 2*c*), plagioclase feldspar (Fig. 2*d*), magnetite and ilmenite. Apatite is associated with some feldspar and amphibole megacrysts. A single olivine megacryst (that could be derived from a xenolith) was noted in D1C1. Table 1 lists the megacryst assemblages found in the individual samples. All megacrysts form prominent grains much coarser than the minerals in the lavas. Pyroxene, amphibole and feldspar appear resorbed: amphibole and feldspar commonly show reaction coronae with the lava matrix and/or have been reduced to ellipsoidal outlines. The opaque oxides in contrast occur as large equant grains that

Table 1: Summary of xenolith and megacryst petrography in Funk Seamount lavas.

Sample	Amph	Cpx	Opx	Mt	Ilm	Ol	Plag	Ap
Xenoliths								
D1A1	x	x	x			x		x
D1A2	x	x	x	x				
D1B2	x	x		x	x	x		
D1C1	x	x	x	x	x	x		
D1C2	x	x	x	x	x		x	
Megacrysts								
D1A1	x	x	x	x	x		x	
D1A2	x			x			x	
D1B1	x	x		x	x		x	x
D1B2	x			x	x		x	
D1C1	x	x		x	x	x	x	
D1E	x	x		x	x		x	

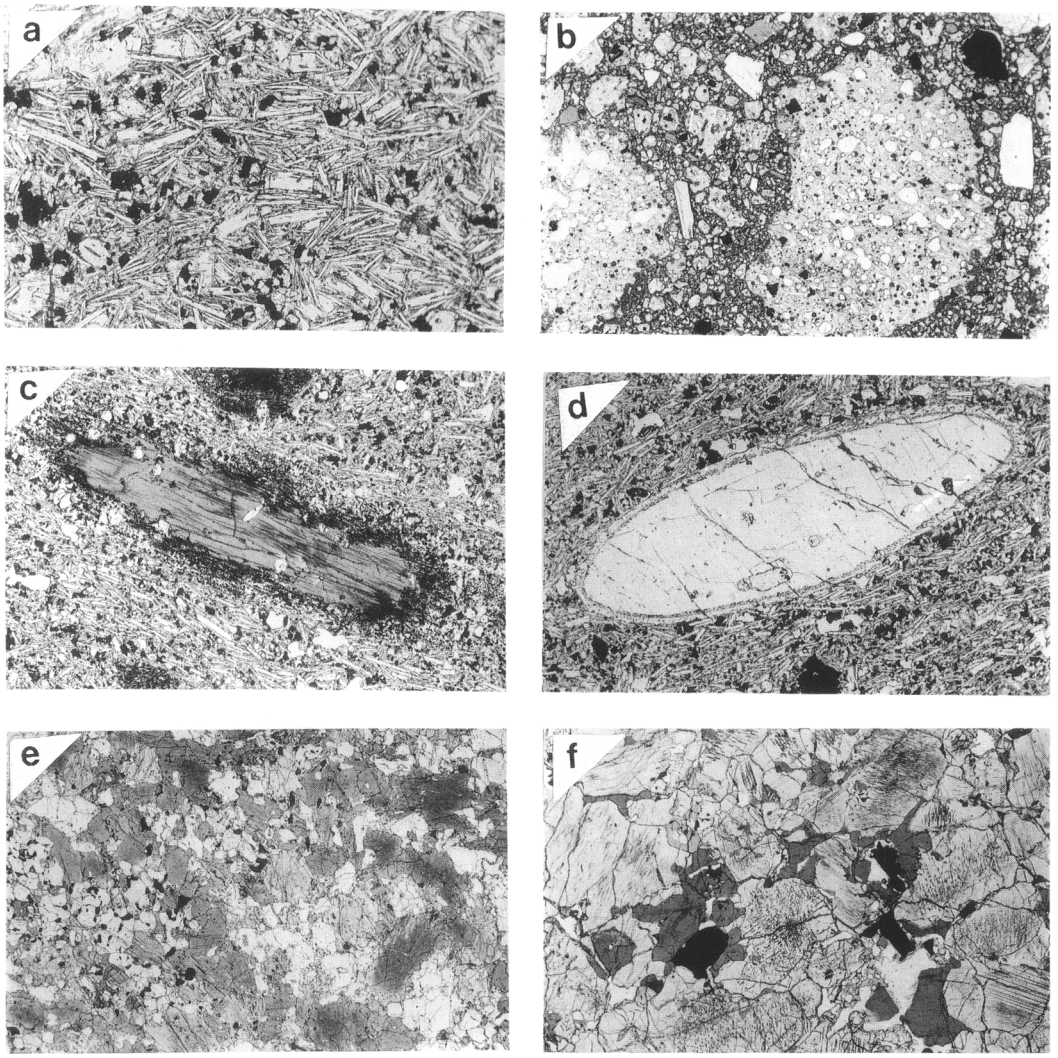

FIG. 2. Photomicrographs in plane polarised light showing: (*a*) Matrix feldspars in lava D1A2 showing flow alignment. Field of view (FOV) = 1.35 mm; (*b*) Glassy lava fragments in breccia sample D1A1. FOV = 3.4 mm; (*c*) Partially resorbed amphibole megacryst in lava sample D1B2. FOV = 3.4 mm; (*d*) Rounded plagioclase megacryst showing reaction rim in lava sample D1B2. FOV = 3.4 mm; (*e*) Xenolith sample D1C2 comprising amphibole, clino- and orthopyroxene, plagioclase and FeTi oxides. FOV = 6.8 mm; (*f*) Amphibole peridotite xenolith in lava sample D1C1 showing amphibole (dark), clinopyroxene with exsolution lamellae of FeTi-oxides and single large titanomagnetite crystals. FOV = 6.8 mm.

may have overgrowths but show little evidence of reaction with the host lava.

The xenoliths are generally small with clean 'abraded' margins that only locally show reaction with the matrix. Sample D1C2 (Fig. 2*e*) comprises a single large (0.2 kg) xenolith with a similar mineral assemblage to those included in the lavas, but with plagioclase as an additional phase. Mineral assemblages vary (see Table 1 for a list of assemblages), as do mineral abundances. The size and number of xenoliths is too small to allow any generalizations. They are all brown amphibole–pyroxene rocks generally either with olivine or with plagioclase (Fig. 2*f*). Opaque oxides (magnetite and ilmenite) occur in most xenoliths. D1A1 lacks abundant opaques and has significant apatite.

The xenoliths show textural evidence of recrystallization. Amphibole replaces pyroxene and vice versa, and some of the pyroxene-amphibole aggregates are partially converted to fine-grained aggregates of fairly equant grains with intergrown sutured margins. Many of the larger pyroxenes show exsolution primarily of lamellae and rods of opaque oxides. Lamellae of amphibole in pyroxene may be due to exsolution or replacement. In addition to recrystallization, which may have taken place at the original site of aggregation or on transport to the surface, the xenoliths show evidence of intergranular decompression melting. Localized pools of clear yellowish glass are common in the interstices of the xenoliths, where the glass coats the adjacent xenolith minerals. Vesicles and euhedral microphenocrysts of pyroxene and olivine occur within the glass which shows a range of composition. The glass and enclosed microphenocrysts are interpreted as the product of highly localized intergranular melting, followed by rapid crystallization, due to pressure release consequent on disruption of the xenolith parent, and transport up the vent entrained in the basanite magma.

Bulk composition of the lavas

Material was separated from each of the four lava samples for chemical analysis. A diamond corer was utilized for sampling in an attempt to avoid the megacrysts and xenoliths and obtain a relatively uncontaminated lava sample. The resultant X-Ray fluorescence analyses, using the procedures outlined in le Roex and Dick (1981), are presented in Table 2. The four lava samples are very similar in bulk composition and could even be from the same flow. All are Ti and alkali rich basalts with

Table 2: Bulk rock and glass analyses of Funk Seamount lavas, glasses and xenoliths. FeO* = total iron as FeO. Mg#=atomic Mg/Mg+Fe^{2+} (Fe_2O_3/FeO assumed=0.20)

	1	2	3	4	5	6	7	8	9	10	11
	D1A2 Lava	D1B1 Lava	D1B2 Lava	D1E Lava	D1A1 glass clast	D1C1 glass clast	D1C2 xeno.	D1C1 glass xeno.	D1C1 glass xeno.	D1C2 glass xeno.	D1C2 glass xeno.
SiO_2	44.38	44.69	44.33	44.94	48.01	48.66	44.41	46.91	48.33	44.38	44.48
TiO_2	3.99	4.05	3.92	4.01	3.64	4.13	2.93	3.84	4.00	3.34	3.22
Al_2O_3	16.08	16.03	16.08	16.10	16.26	16.50	14.16	17.32	17.05	15.79	15.32
FeO*	13.41	13.59	13.24	13.53	11.13	11.40	12.36	10.98	11.12	13.86	13.66
MnO	0.16	0.16	0.16	0.15	0.17	0.18	0.16	0.06	0.19	0.16	0.15
MgO	5.74	5.59	4.86	5.88	3.92	4.04	10.64	4.54	4.81	6.88	7.27
CaO	7.85	8.09	8.31	8.05	8.07	8.61	9.88	9.83	9.75	9.28	9.13
Na_2O	4.77	4.65	4.29	4.37	3.58	3.29	2.58	3.58	3.65	3.08	3.10
K_2O	1.62	1.66	1.64	1.69	2.32	2.28	0.70	0.73	0.64	1.30	1.30
P_2O_5	1.07	1.10	1.13	1.08	1.40	-	0.48	-	-	-	-
LOI	1.13	0.79	1.97	0.77	-	-	1.72	-	-	-	-
H2O-	0.16	0.13	0.37	0.14	-	-	0.20	-	-	-	-
Total	100.54	100.71	100.48	100.89	98.50	99.09	100.38	97.79	99.54	98.07	97.63
Zr	377	379	372	390	-	-	145	-	-	-	-
Nb	59	59	58	62	-	-	34	-	-	-	-
Y	37	38	36	37	-	-	29	-	-	-	-
Rb	21	26	28	29	-	-	3.4	-	-	-	-
Ba	399	391	389	374	-	-	187	-	-	-	-
Sr	1155	1099	1154	1074	-	-	604	-	-	-	-
Co	46	48	49	44	-	-	60	-	-	-	-
Cr	73	73	60	73	-	-	403	-	-	-	-
Ni	44	49	44	41	-	-	236	-	-	-	-
V	177	187	176	175	-	-	256	-	-	-	-
Zn	140	141	140	147	-	-	121	-	-	-	-
Cu	17.9	17.8	16.0	16.9	-	-	34	-	-	-	-
Sc	12.5	12.8	12.0	13.8	-	-	27	-	-	-	-
Zr/Nb	6.4	6.4	6.4	6.4	-	-	4.5	-	-	-	-
Y/Nb	0.63	0.64	0.62	0.61	-	-	0.11	-	-	-	-
Ba/Nb	6.8	6.6	6.7	6.1	-	-	5.8	-	-	-	-
Mg#	0.47	0.46	0.44	0.48	0.43	0.43	0.64	0.47	0.48	0.51	0.53

Analyses 1-4: Bulk rock XRF analyses of lava samples.
5-6: Electron microprobe analyses of basaltic glass breccia clasts.
7 : Bulk rock XRF analysis of a large xenolith.
8-11: Electron microprobe analyses of interstitial glass in xenoliths.

8–11% normative nepheline and are classed as basanitoids.

Comparison of incompatible trace element ratios least affected by alteration and near-surface fractionation (e.g. Zr/Nb, Y/Nb, Ba/Nb) shows that the Funk Seamount lavas are similar to the Marion and Prince Edward Island lavas. For example, Funk Seamount lavas have Zr/Nb, Y/Nb and Ba/Nb ratios of 6.4, 0.62 and 6.6 respectively, while comparable ratios from Marion Island are 6.6, 0.60 and 7.8 respectively, and those from Prince Edward Island are 8.4, 0.72, and 6.7 respectively (le Roex, unpubl. data; Kable *et al.*, 1971). The $^{87}Sr/^{86}Sr$ ratio of sample D1A2 is 0.703237 ± 14 which is intermediate between those for Marion and Prince Edward Islands (0.70339 and 0.70307 respectively; Hart, unpubl. data). The $^{143}Nd/^{144}Nd$ ratio of sample D1A2 is 0.513020 ± 9, again similar to, although slightly higher than those for Marion and Prince Edward Islands (0.51291 and 0.51297 respectively; Hart, unpubl. data). These data, taken in conjunction with the trace element ratios and spatial association, suggest that the Funk Seamount lavas have derived from a similar mantle source region to that giving rise to the Marion and Prince Edward hotspot lavas.

Also presented in Table 2 are analyses of basaltic material from the volcanic breccias. These are electron microprobe analyses of the glass from the plagioclase–olivine vitrophyres that are the major clast type. Compared to the lavas these are also melts high in Ti and alkalis but with higher silica and lower Mg. Mg# [atomic $Mg/(Mg+Fe^{2+})$; $Fe_2O_3/FeO = 0.20$] is 0.34–0.39 compared with

Table 3: Selected compositions of minerals in Funk Seamount lavas and xenoliths. Fe_2O_3 reported for Fe-Ti oxides has been calculated on the basis of stoichiometry.

Type	Lava	Glass clast	Xeno.	Xeno.	Lava	Xeno.	Xeno.	Mega.	glass xeno.	Xeno.	Xeno.	Mega.	Xeno.	Xeno.	Xeno.	Mega.	Mega.
Sample	D1E	D1C1	D1C1	D1A1	D1B2	D1C1	D1C2	D1A1	D1C2	D1C1	D1C2	D1A1	D1C1	D1A1	D1C2	D1A1	D1B1
	Ol	Ol	Ol	Ol	Cpx	Cpx	Cpx	Cpx	Cpx	Opx	Opx	Opx	Amph	Amph	Amph	Amph	Amph
SiO_2	37.91	37.77	37.41	37.50	50.44	49.51	50.67	49.57	49.99	53.65	52.20	52.47	40.45	42.31	40.96	39.32	39.18
TiO_2	-	-	-	-	2.06	1.10	0.53	1.21	1.15	0.20	0.16	0.21	3.73	3.55	3.18	4.51	5.20
Al_2O_3	-	-	-	-	3.03	5.39	3.47	6.30	5.60	3.84	2.12	3.66	13.88	12.66	12.62	14.31	14.21
Cr_2O_3	-	-	-	-	0.02	0.11	0.12	0.25	0.08	-	-	-	0.13	0.12	0.07	-	-
FeO	22.86	23.34	27.88	25.71	8.13	8.37	8.75	7.39	8.27	15.47	20.22	16.17	10.80	9.85	13.70	15.05	14.04
MnO	0.23	0.24	0.34	0.29	0.14	0.22	0.30	0.12	0.18	0.23	0.59	0.34	0.13	0.07	0.18	0.18	0.12
MgO	38.71	38.26	34.26	36.40	14.15	13.58	13.54	13.52	13.92	26.61	23.46	25.27	13.87	14.29	12.34	10.47	10.59
CaO	.09	.13	.14	.08	21.60	20.71	21.37	20.73	19.28	0.58	0.68	0.62	11.34	11.64	11.33	10.88	10.97
Na_2O	-	-	-	-	0.50	0.74	0.82	0.54	0.70	-	0.08	-	2.91	2.71	2.49	2.97	2.79
K_2O	-	-	-	-	-	-	-	-	-	-	-	-	0.72	0.89	1.10	0.95	1.06
NiO	0.07	-	0.09	-	-	-	-	-	-	-	-	-	-	-	-	-	-
Total	99.87	99.75	100.13	99.98	100.07	99.75	99.59	99.64	99.17	100.59	99.52	98.76	97.96	98.09	97.97	98.65	98.17
Fo	75.1	74.5	68.7	71.6	Wo 45.4	44.9	45.4	45.8	42.8	1.2	1.4	1.3					
Fa	24.9	25.5	31.4	28.4	En 41.3	40.9	40.0	41.5	42.9	74.5	66.5	72.6					
					Fs 13.3	14.2	14.5	12.7	14.3	24.3	32.2	26.1					

Type	Mega.	lava	lava	Glass clast	Xeno.	Mega.	Mega.	Xeno.	Xeno.	Mega.	Mega.	Lava	Glass clast	Xeno.	Xeno.	Mega.	Mega.
Sample	D1E	D1A2	D1B2	D1A1	D1C2	D1A2	D1B1	D1C1	D1B2	D1A1	D1B1	D1A2	D1A1	D1C1	D1C2	D1E	D1B2
	Amph	Fsp	Fsp	Fsp	Fsp	Fsp	Fsp	Ilm	Ilm	Ilm	Ilm	Mgt	Mgt	Mgt	Mgt	Mgt	Mgt
SiO_2	39.95	52.54	52.96	52.11	57.87	60.19	56.50	-	-	-	-	0.12	0.11	-	-	-	0.11
TiO_2	5.39	-	-	-	-	-	-	48.73	51.67	45.15	48.51	22.16	18.46	13.71	21.84	16.27	14.21
Al_2O_3	14.08	28.80	29.15	29.84	26.62	24.81	27.43	0.73	0.48	0.46	0.57	1.95	7.13	6.09	6.82	6.21	6.80
Cr_2O_3	-	-	-	-	-	-	-	0.25	0.56	-	-	0.02	-	0.54	0.64	-	0.05
Fe_2O_3	-	-	-	-	-	-	-	11.31	7.63	16.32	10.81	24.63	27.68	36.43	21.55	32.77	35.31
FeO	13.77	0.74	0.83	0.69	0.13	0.15	0.19	31.02	32.28	34.86	34.18	47.05	40.39	38.52	40.43	39.69	38.52
MnO	0.16	-	-	-	-	-	-	0.36	0.35	0.34	0.33	0.69	0.25	0.40	0.30	0.37	0.25
MgO	11.30	-	0.10	0.14	-	-	-	6.98	7.76	3.01	5.11	2.63	5.73	3.74	7.49	4.67	4.35
CaO	9.63	12.77	11.51	12.39	8.51	6.23	9.20	-	-	-	-	0.13	0.07	-	-	-	-
Na_2O	3.30	3.90	4.52	3.84	6.71	7.50	5.78	-	-	-	-	-	-	-	-	-	-
K_2O	0.92	0.27	0.31	0.24	0.34	0.53	0.35	-	-	-	-	-	-	-	-	-	-
Total	98.51	99.02	99.38	99.42	100.18	99.42	99.45	99.38	100.73	100.16	99.51	99.38	99.82	99.43	99.07	99.99	99.60
		Or 1.6	1.8	1.5	1.9	3.1	2.1										
		Ab 35.0	40.8	35.4	57.7	66.4	52.1										
		An 63.4	57.4	63.1	40.4	30.5	45.8										

0.43–0.47 in the basanitoids. The glasses are alkali olivine basalts with a trace of nepheline in the CIPW norm. Electron microprobe analyses of decompression melts in the xenoliths (Table 2) show them to be compositionally variable but remarkably similar to both the basanitoid lavas (e.g. glass in D1C2) and to the alkali olivine basalt glasses (e.g. glass in xenoliths in D1C1), although with somewhat lower K_2O contents.

Mineral chemistry

Mineral phases have been analysed by a Cambridge Microscan V electron microprobe with on-line reduction following the procedures outlined in le Roex and Dick (1981). Representative mineral analyses are given in Table 3 and selected mineral data are plotted in Figs. 3 to 6. Individual mineral analyses can be obtained from the authors on request.

Lavas. Olivine phenocrysts and microphenocrysts in the basanitoid lavas have a limited compositional range, $Fo_{70.0-75.6}$ with Fo_{75} as the dominant composition. CaO content averages 0.20 wt.% (range 0.09 to 0.38) and MnO averages 0.26 wt.% (range 0.20 to 0.35). Olivines occurring as microphenocrysts in the glassy alkali olivine basalts (glassy clasts in breccias) show a very narrow compositional range essentially similar to the more magnesian olivines in the basanitoids (Fo_{74-75}). CaO contents range from 0.1 to 0.36 wt.% (average 0.23) and MnO ranges from 0.22 to 0.32 wt.% (average 0.27). Nickel contents in both groups of olivines are low (< 0.1 wt.% NiO).

Plagioclase laths in the basanitoid lavas are labradorites (Fig. 3). They range in anorthite con-

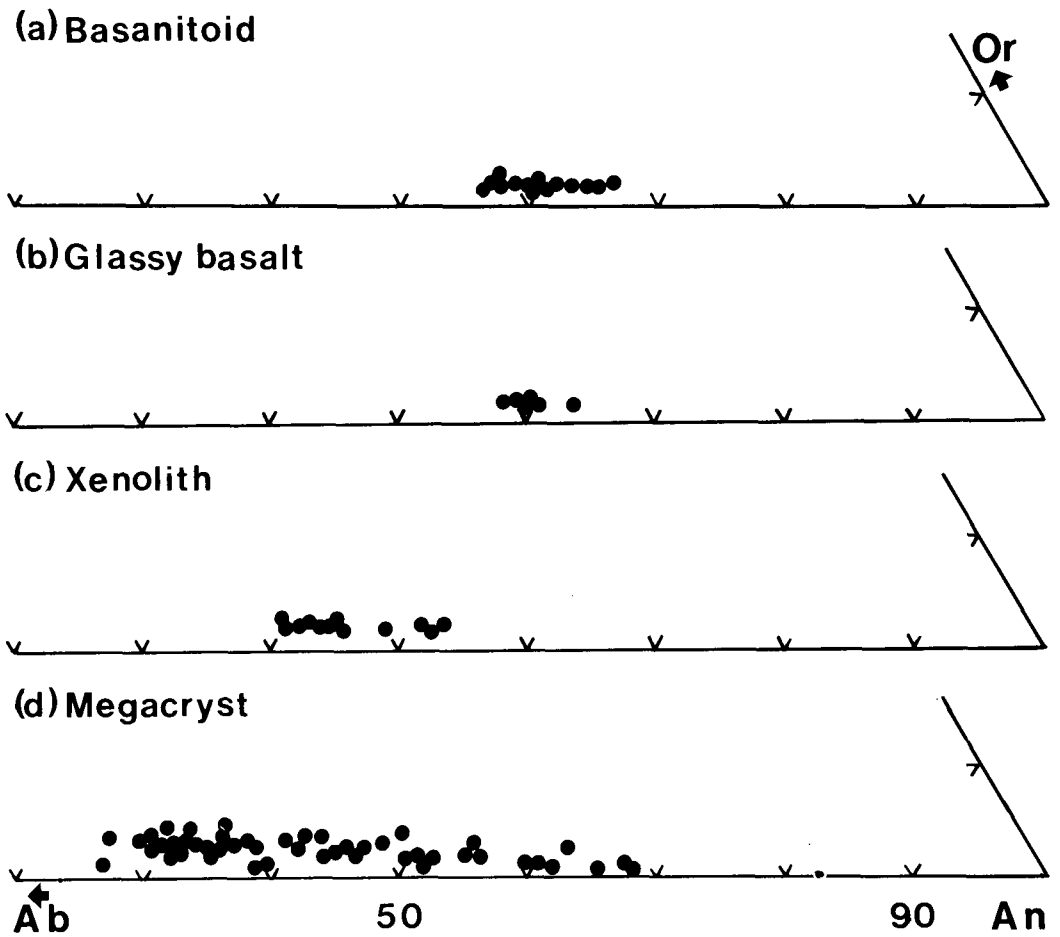

FIG. 3. Feldspar compositions in Funk Seamount lavas, vitrophyres, xenoliths and megacrysts.

tent from An_{56} to An_{66} with 1.5–2 mol.% K-feldspar and 0.5 to 1.0 wt.% FeO. Plagioclase microphenocrysts in the glassy clasts are also labradorites, similar in composition at An_{57-60}, with 1.7–2.1 mol.% K-feldspar and FeO around 0.8 wt.%.

Pyroxene occurs in the basanitoids as Ca-rich clinopyroxenes with compositions clustering around $Wo_{45}En_{42}Fs_{13}$ (Fig. 4). The pyroxenes have 2–2.3 wt.% TiO_2, 2.7–3 wt.% Al_2O_3 and 0.4–0.5 wt.% Na_2O. No pyroxene was detected in the glassy clasts.

Small opaque grains analysed in the lavas are almost entirely titaniferous magnetite (Fig. 5*a*) with 20–24 wt.% TiO_2 and significant MgO (2.5–5 wt.%) and Al_2O_3 (2–7 wt.%). A single ilmenite grain in D1B1 gave an analysis of $Ilm_{74}Gk_{15}Hem_{11}$ which, in conjunction with the magnetite gives a temperature (Buddington and Lindsley, 1964) of around 1100 °C at an oxygen fugacity equivalent to the quartz-fayalite-magnetite buffer. The opaque microphenocrysts in the glassy clasts are also mostly magnetite with 17–22 wt.% TiO_2, 6–8 wt.% Al_2O_3 and around 6 wt.% MgO. Rare ilmenites have higher MgO, equivalent to 22% geikelite molecule, and yield a temperature also around 1100 °C at a slightly higher f_{O_2} (approximately 10^{-9}) than for the basanitoids.

Megacryst suite. The abundant megacryst pyroxene is a clinopyroxene ($Wo_{45-49}En_{43-38}Fs_{11-15}$) with an average TiO_2 content of 1.3 wt.% (range 1.0–1.7), average Al_2O_3 of 6.4 wt.% (range 5.3–7.4) and average Na_2O of 0.6 wt.% (range 0.4–1.0). These values closely match the

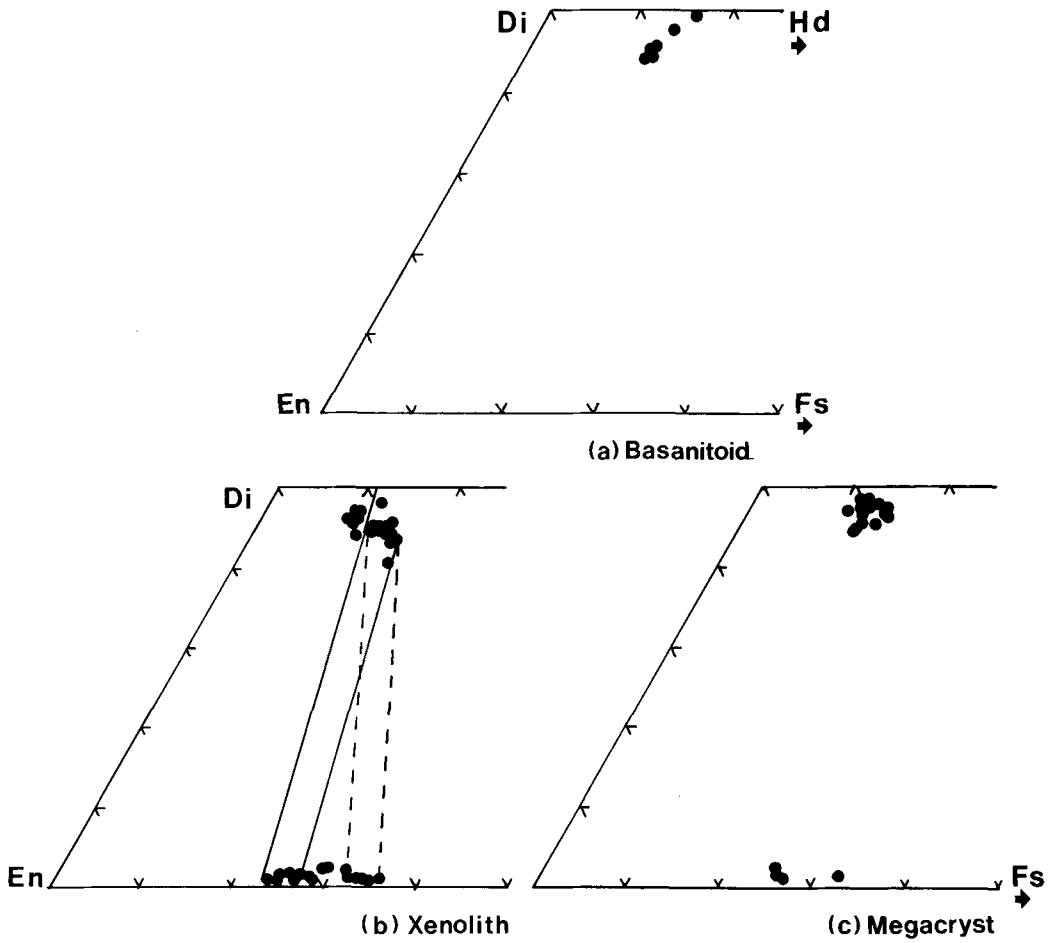

FIG. 4. Pyroxene compositions in terms of quadrilateral components in Funk Seamount lavas, xenoliths and megacrysts. Tie lines show coexisting pyroxene compositions in D1C1 (solid) and D1C2 (dashed).

pyroxenes in the basanitoids (Fig. 4), with the megacryst pyroxenes generally having slightly higher CaO, higher Al_2O_3, and less TiO_2. Orthopyroxene megacrysts were found only in the glassy breccia D1A1. Their composition is equivalent to $Wo_{1.3-2.3}En_{73}Fs_{25}$ (with one more iron-rich grain $Wo_{1.9}En_{66}Fs_{32}$) with much lower TiO_2 (0.1–0.3 wt.%) and Al_2O_3 (2.7–3.7 wt.%) than the megacryst clinopyroxenes. Some show narrow clinopyroxene exsolution lamellae. The megacryst amphibole is a kaersutite with high ^{IV}Al and Ti. The TiO_2 content averages 4.8 wt.% (range 3.8–5.6) and atomic $Mg/(Mg+Fe^{2+})$ averages 0.58 (range 0.56–0.62).

In contrast to the mafic megacrysts, plagioclase megacrysts embrace a wide compositional range (Fig. 3). The more calcic compositions match those in the basanitoids and alkali olivine basalts ranging up to An_{66}. The megacryst feldspars however show a fairly continuous trend of increasing Na up to An_{26}, with the more sodic compositions being the more abundant. Megacryst feldspars form therefore a series from labradorite to oligoclase and have either crystallized from a series of fractionated melts or represent different stages in the re-equilibration of sodic plagioclase grains caught up in a basaltic matrix where calcic labradorite is the stable phase. The latter alternative seems less likely in view of the lack of zoning and the presence of well defined reaction rims around essentially unzoned grains. Also molar orthoclase correlates well with Na content, rising from 0.7 to 4.2%. The FeO content is lower than for the basaltic feldspars, ranging from 0.1 to 0.4 wt.% (average 0.19).

The majority of the opaque megacrysts are titaniferous magnetites with 14.2–21.1 wt.% TiO_2 (average 16.1) and MgO contents ranging from 1.6 to 6.7 wt.% (average 4.2). In terms of end-member molecules, most lie between 9 and 17 mol.% spinel, 38–47% ulvospinel and 41–49% magnetite (Fig. 5*a*). Less abundant are ilmenite megacrysts with 38.8–48.5 wt.% TiO_2 (average 44.4) and 3.2–6.4 wt.% MgO (average 4.9). These recalculate to 10–23% geikelite, 54–71% ilmenite and 9–28% hematite in terms of end-member molecules (Fig. 5*b*).

Oxide phases also occur within the megacrysts as very thin lamellae in pyroxene. Analysis of one such lamella gave a composition intermediate between magnetite, ulvöspinel and spinel but with 6.7 wt.% Cr_2O_3 ($Mt_{38}Sp_{32}Usp_{21}Chr_7$).

Xenolith suite. Clinopyroxenes in the xenoliths have a restricted compositional range ($Wo_{41-49}En_{40-45}Fs_{10-17}$) and closely resemble the lava and megacryst clinopyroxenes (Fig. 4). TiO_2 contents in xenolith clinopyroxenes are somewhat lower (range 0.5–1.4, average 0.94 wt.%) than the average megacryst (1.3 wt.%) or average lava pyroxene (2.1 wt.%). Xenolith clinopyroxenes average 4.98 wt.% Al_2O_3 (range 3.2–6.2), lower than those in the megacryst suite (5.3–7.4 wt.%), but higher than lava pyroxenes (2.7–3 wt.%). Clinopyroxenes in the more iron-rich xenolith D1C2 are at the lower end of this range, averaging 3.6 wt.% Al_2O_3. Average Na_2O of the xenolith pyroxenes is 0.60 wt.%.

Xenolith orthopyroxenes are compositionally similar to those occurring as megacrysts (Fig. 4); they cover the range $Wo_{1-2}En_{71-76}$ with D1C2 orthopyroxene being more iron-rich at $Wo_{1-2}En_{64-67}$. TiO_2 contents (0.05–0.43 wt.%, average 0.18) are comparable to the megacrysts but Al_2O_3 contents (1.6–3.8 wt.%, average 2.60) are lower than the megacrysts (approx. 3.5 wt.%). As with the clinopyroxenes, D1C2 orthopyroxene is at the lower end of this range (average 2.1 wt.%). Feldspar is generally absent in the xenolith suite, but is prominent in the D1C2 xenolith where it is andesine (An_{40-49}) with low K_2O (mol.% K-feldspar 1.7–2.1).

Amphibole is present in all the xenoliths and is compositionally similar to the megacryst kaersutites. Compared to the megacryst amphiboles, however, TiO_2 is lower (average 3.5 wt.% versus 4.8 in the megacrysts) and the xenolith amphiboles are more correctly classified as Ti-rich pargasites rather than kaersutites (Leake, 1978). Most xenolith amphiboles have atomic $Mg/(Mg+Fe^{2+})$ around 0.69 compared to the megacrysts at 0.58. D1C2 amphibole has $Mg/(Mg+Fe^{2+})$ of 0.61, slightly lower CaO and higher K_2O than the other xenolith amphiboles.

Magnetites in the xenoliths are titaniferous (average 15.8 wt.% TiO_2) and have significant contents of Al_2O_3 (5.1–7.1 wt.%) and MgO (3.5–7.5 wt.%). They are similar to megacryst magnetites but range to somewhat higher TiO_2 contents (Fig. 5*a*). Xenolith ilmenite has 11–22 mol.% geikelite (MgO 5.6–9.0 wt.%) and high calculated hematite contents, as with the megacrysts (Fig. 5*b*). The xenoliths contain more high-Mg ilmenites than the megacrysts.

Three xenoliths examined carry olivine, ranging in composition from Fo_{72} to Fo_{66} with low CaO (around 0.15 wt.% but lower in the more magnesian olivines) and NiO (around 0.1 wt.%) contents. Apatite in the xenolith suite was not analysed.

Summary and comparison of the mineral chemistry. Fig. 4 is a comparison among the various pyroxenes. In terms of quadrilateral components, the lavas, megacryst suite and xenoliths have very similar pyroxene, except that the lavas have only a high-Ca pyroxene. The clinopyroxenes are all extremely similar with the xenolith clinopyroxenes showing slightly more scatter. This is also true for the orthopyroxenes: orthopyroxenes have been found as isolated coarse grains (megacrysts) only in

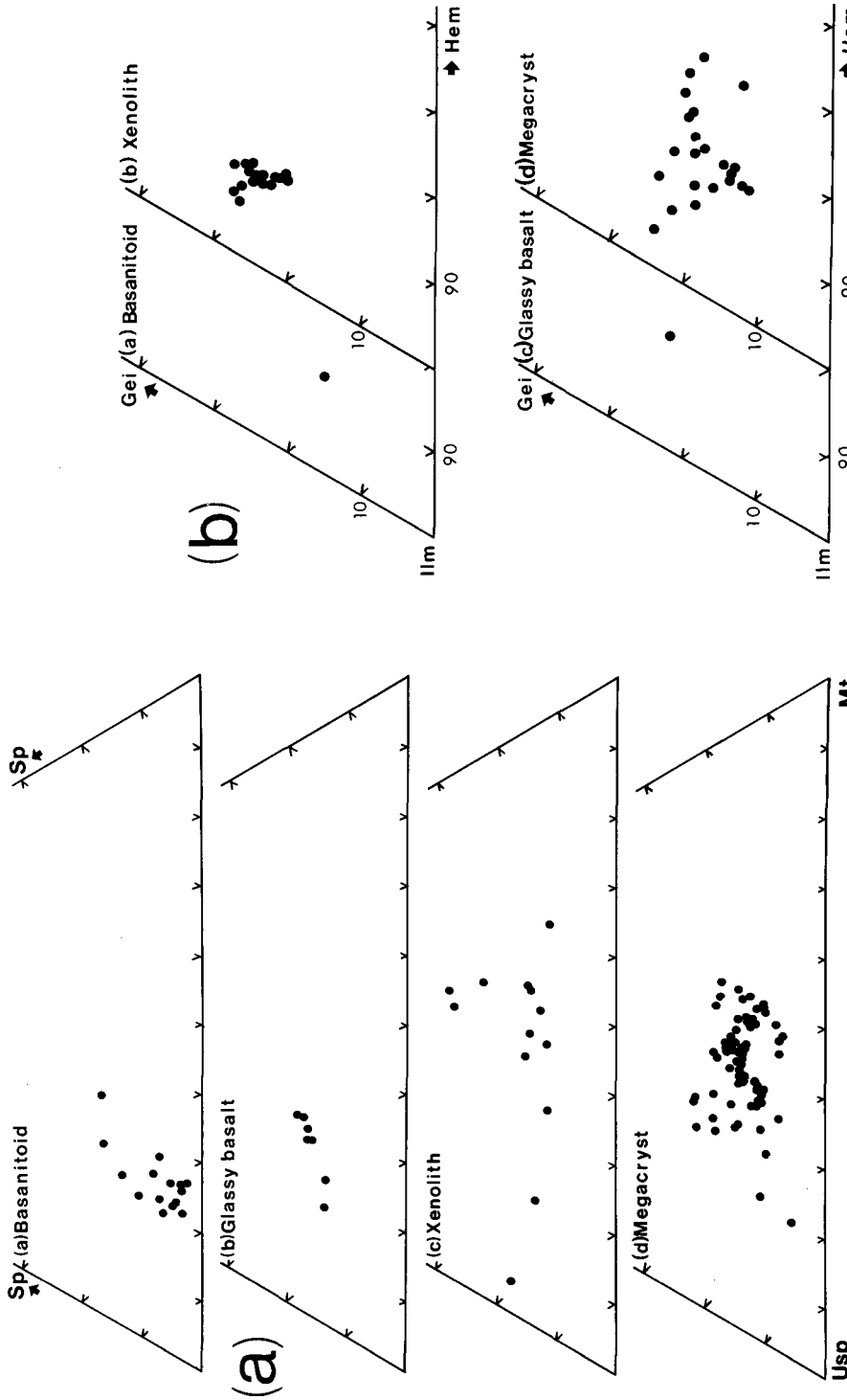

FIG. 5 (*a*) Titanomagnetite compositions in terms of spinel, ulvöspinel and magnetite components in Funk Seamount lavas, vitrophyres, xenoliths and megacrysts. (*b*) Ilmenite compositions in terms of ilmenite, hematite and geikelite components in Funk Seamount lavas, vitrophyres, xenoliths and megacrysts.

D1A1 where they have a limited spread of compositions. In contrast, the xenolith orthopyroxenes show a greater spread of values: this is illustrated in Fig. 4, where tie lines have been drawn between groups of coexisting pyroxenes for different xenoliths. The orthopyroxenes in the D1C2 xenolith are more iron-rich than the others but the tie lines are essentially parallel to those for D1A1 and D1A2. The D1C1 xenolith has more magnesian orthopyroxene, consistent with a higher equilibration temperature and a different slope to the tie lines.

Triangular plots of Na–Ti–^{IV}Al are similar for megacryst and xenolith pyroxenes (the latter showing more scatter), and indicate that most of the Al can be accounted for as substitution of Tschermak's molecule with relatively minor substitution of jadeite and a coupled Ti–Al substitution. The Ti–Al and Al–Al substitution are however linked, as plots of Ti versus total Al show strong positive correlations with the same slope in both megacryst and xenolith pyroxenes (Fig. 6). Among the xenoliths, D1C1 has the most aluminous pyroxenes whereas D1C2 pyroxenes, which coexist with feldspar, are significantly less aluminous. The megacryst clinopyroxenes extend to even higher Al contents and have no lower Al values comparable to the xenolith pyroxenes in D1C2.

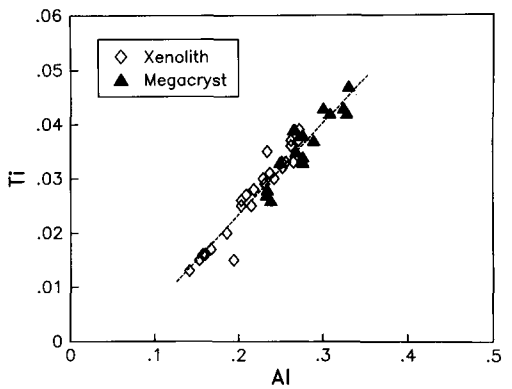

FIG. 6. Atomic Ti versus total atomic Al in Funk Seamount xenolith and megacryst clinopyroxenes.

Fig. 3 contrasts the feldspar composition in the various suites. The lava feldspars show a restricted compositional range, as does feldspar from the one feldspar-bearing xenolith, which is significantly more sodic than the groundmass feldspar in the lava. In contrast, the megacryst plagioclase shows a very wide compositional spread, from oligoclase to calcic labradorite. Each sample contains a range of feldspar megacryst compositions but in samples analysed there is a tendency for the megacrysts in the basanitoids to be more sodic than those in the glassy alkali basalts.

In composition and occurrence the brown amphiboles match the high-Ti and K/Na, low-Mg/Fe and Cr amphiboles that occur in group II xenoliths, as veins in xenoliths and as megacrysts (Wilkinson and le Maitre, 1987). Interstitial amphiboles in group I xenoliths have higher Mg/Fe and Cr, and much lower Ti (Wilkinson and le Maitre, 1987). Megacryst and xenolith amphibole are very similar to megacrysts forming a tighter cluster, at somewhat higher Na contents. Xenolith amphiboles range in Al in like manner to the pyroxenes, higher in xenolith D1C1, lower in feldspar-bearing D1C2. The greater spread in composition of xenolith phases in comparison with megacrysts is also noted for the titaniferous magnetites and the ilmenites, which show a much greater range in 'calculated' Fe^{2+}/Fe^{3+} ratios for the xenoliths (Fig. 4). Xenolith olivines have lower Ca contents (< 0.15 wt.%) and a wider range of Mg/Fe ratios, stretching to lower Fo contents (66–72) than olivine in the lavas (CaO 0.20–0.35 wt.%; Fo_{70-76}).

The general similarities in phase compositions for these different suites of minerals are consistent with derivation from a common parent melt or from a series of closely related magmas. The megacrysts (except for plagioclase) show a remarkably limited compositional spread. Xenolith assemblages indicate derivation from a greater range of environments with D1C2 as the more fractionated (or less depleted) feldspathic assemblage. The range in xenolith phase compositions probably represents different degrees of compositional adjustment to lower temperature–pressure environments. The xenolith D1C1 has the least modified texture and mineralogically is the highest temperature–pressure assemblage.

Origin of the xenoliths

The xenoliths exhibit a range of mineral assemblages and of modal abundances, but with a limited range of mineral compositions. This is a not uncommon feature in ultramafic nodules, where the assemblages have equilibrated in similar environments, perhaps with a common melt, but where heterogeneities in bulk composition on a hand-specimen scale are allowed to persist. These conditions could be satisfied if the xenoliths have crystallized from a common melt and aggregated together as a consequence of properties and processes unrelated to those determining chemical equilibria. In this sense the xenoliths could be aggregates, though not necessarily gravity cumulates. The

xenoliths would then be interpreted as random samples of heterogeneous cumulates (aggregates) crystallized at depth from a basanitoid melt. Alternatively the xenoliths could be samples of heterogeneous 'wall rock' that have become entrained in the basanitoid melt. They are not, however, accidental xenoliths but rather, as is argued below, assemblages that were probably in equilibrium at depth with a basanitoid melt. The xenoliths in this sense, then, are residual assemblages, the solid material with which the melt was in equilibrium when it formed at depth.

The xenoliths all have kaersutitic hornblende as a prominent constituent, in sharp contrast to the anhydrous assemblages in the host lavas. Merrill and Wyllie (1975) have investigated the conditions under which kaersutite will crystallize from a melt of basanitic composition. Their experiments were performed on a kaersutite and a kaersutite eclogite from Kakanui, New Zealand. The kaersutite ecologite is compositionally equivalent to a basanite with somewhat higher MgO and lower alkalis than the Funk Seamount basanites. Kaersutite was found to be a liquidus phase in these experiments in the pressure range 11–21 kbar, provided the melt had greater than about 3 wt.% water. Olivine crystallizes from the melt up to around 18 kbar, along with clinopyroxene and amphibole. There is a small primary orthopyroxene field, but only in the range 17–21 kbar at high water contents (> 3 wt.%). The xenolith assemblages from the Funk Seamount are thus consistent with crystallization from a basanitic melt at depth, in the approximate pressure range 17–21 kbar, provided the melt has a high water content. The partitioning of Fe and Mg between olivine and silicate melt ($K_D^{ol-liq} = 0.30$; Roeder and Emslie, 1970) is also consistent with the xenoliths being in approximate equilibrium with a melt similar in composition to that of the basanitoids (calculated values of $K_D = 0.30$–0.34).

We conclude that the kaersutite-bearing xenoliths probably equilibrated with a hydrous basanitic melt at depths around 50–60 km. The assemblages could be 'cumulates', aggregated from the melt, or 'residua' that were in contact with the melt at depth. Xenolith assemblages such as D1C2 have lower Mg/(Mg + Fe) ratios than the other xenoliths and have plagioclase as a major phase. Such assemblages may also have formed in contact with a hydrous basanitic melt but from a more fractionated basanite and in a pressure regime where plagioclase was stable. Such constraints, coupled to the textural evidence, suggest that D1C2 type xenoliths are either cumulates formed at shallower depth than the more magnesian, feldspar-free xenoliths, or are residual assemblages associated with smaller degrees of partial melting. The similarity in composition between the decompression melts in D1C2 and the basanitoids (Table 2) indicates that such an assemblage is capable of producing a basanitic melt on partial melting.

Origin of the megacrysts

The arguments that relate the xenolith assemblages to a basanitic magma at depth can also be applied to the megacryst suite. The megacryst minerals differ from those in the xenoliths in: (1) the absence or near absence of olivine; (2) the abundance of plagioclase (excluding the feldspathic xenolith D1C2); (3) the limited range in mineral composition (except for plagioclase); and (4) the wide range of plagioclase composition. The mineral compositions are also consistent with crystallization from a hydrous basanitic melt at depth. The monomineralic nature of most megacrysts, their large size and homogeneity, and their uniform composition suggest that they were in intimate contact with a homogeneous body of melt and did not aggregate into polymineralic assemblages. We interpret the megacrysts as high-pressure phenocrysts grown in a hydrous basanite melt. By this model the xenoliths, with their wider range of compositions and modal diversity, resemble the megacrysts because they have been in contact with similar magma but differ from them in that they represent 'magma chamber wall-rock' rather than primary crystals from the melt. Olivine could then be a common phase in the residue but not in the primary crystallites.

The role of feldspar is different from that of the other megacrysts in that a wide range of compositions occurs. The more sodic compositions form abundant large unzoned grains with pronounced 'fingerprint' texture where in contact with the basanite host. Sodic plagioclase and anorthoclase are fairly common megacryst phases in alkali basalts (e.g. Aoki, 1970; Laughlin *et al.*, 1974). Such plagioclase megacrysts have been interpreted as high-pressure phenocrysts and available experimental evidence interpreted as favouring more sodic plagioclase as pressure increases (Aoki, 1970; Binns, 1969; Laughlin *et al.*, 1974). The large oligoclase megacrysts would by this token represent crystallization at the highest pressures (20–23 kbar according to the expression given by Nash, 1973), in association with the other megacryst phases.

The range of plagioclase compositions could then represent the product of continued feldspar crystallization with pressure decrease, as the melt ascends. If this is the case, then only feldspar in the megacryst assemblage represents crystallization over a broad range of physical environments,

whereas the other megacryst phases could derive from a narrow P–T regime, or be less sensitive to changes in physical conditions. The density of plagioclase, over the pressure range involved, more closely matches magma density than do the other phases (Deer *et al.*, 1966) and may contribute to the relative abundance of feldspar megacrysts in alkalic basalts.

Thus we conclude that feldspar also crystallized at considerable depth from the basanitic melt, as a sodic plagioclase. Either some of the early sodic plagioclase reacted with the melt at lower pressures to produce a more calcic feldspar, or, more probably, feldspar continued to crystallize with decreasing pressure as a more calcic plagioclase that was entrained preferentially into the ascending magma.

Summary

Basanitoids and alkali olivine basalts, geochemically similar to the Marion Island volcanics, associated with the Marion Island hotspot, have been recovered from the Funk Seamount to the NW of Marion Island. Xenoliths and megacrysts contained within these alkali volcanics are interpreted as polymineralic aggregates and monomineralic phenocrysts that were in contact with basanitic magma at depth. The abundant presence of kaersutite and its association with other phases implies the formation of a hydrous melt at depths estimated to be around 50–60 km.

The Funk Seamount lavas, as argued above, derive from a similar mantle source region as that giving rise to the Marion and Prince Edward hotspot lavas. The geochemical signature of these lavas implies derivation from a source that is enriched (Ti, K, P, Nb, etc.) over the depleted mantle source regions for the adjacent mid-ocean ridge basalts. The mineralogical evidence of the xenoliths and megacrysts, indicates that kaersutite and apatite (but not mica) are present as stable phases in the source region, at least in the period immediately preceding eruption.

Acknowledgements

We would like to thank H. W. Bergh for making these samples available to us and to Captain Leith and his crew of the S.A. Agulhas for their assistance during dredging. Subsequent work on the samples was supported by the University of Cape Town, the South African Scientific Committee for Antarctic Research, and the Foundation for Research Development of the South African Council for Scientific and Industrial Research. A. B. Simpson is thanked for his assistance with electron microprobe work and J. Harmer for doing the isotopic analyses. A portion of this work was done when the first author was a visiting scientist at the Lunar and Planetary Institute, which is operated by the Universities Space Research Association under contract NASW-4066 with the National Aeronautics and Space Administation. This paper is Lunar and Planetary Institute contribution 638.

References

Aoki, K. (1970) Andesine megacrysts in alkaline basalts from Japan. *Contrib. Mineral. Petrol.* **25,** 284–8.

Binns, R. A. (1969) High pressure megacrysts in basanitic lavas from Armidale, New South Wales. *Am. J. Sci.* **267,** 33–49.

Buddington, A. F., and Lindsley, D. M. (1964) Iron–titanium oxide minerals and synthetic equivalents. *J. Petrol.* **5,** 310–57.

Deer, W. A., Howie, R. A., and Zussman, J. (1966) An introduction to the rock forming minerals. 528 pp. (Longman).

Kable, E. J. D., Erlank, A. J., and Cherry, R. D. (1971) Geochemical features of lavas. Chapter 6 in *Marion and Prince Edward Islands* (E. M. van Zinderen Bakker, J. M. Winterbottom, and R. A. Dyer, eds.). Balkema, Cape Town.

Laughlin, A. W., Manzer, G. K., and Carden, J. R. (1974) Feldspar megacrysts in alkali basalts. *Geol. Soc. Am. Bull.* **85,** 413–16.

Leake, B. E. (1978) Nomenclature of amphiboles. *Am. Mineral.* **63,** 1023–62.

le Roex, A. P., and Dick, H. J. B. (1981) Petrography and geochemistry of basaltic rocks from the Conrad fracture zone on the America–Antarctica Ridge. *Earth Planet. Sci. Lett.* **54,** 117–38.

Merrill, R. B., and Wyllie, P. J. (1975) Kaersutite and kaersutite eclogite from Kakanui, New Zealand—water excess and water deficient melting to 30 kilobars. *Geol. Soc. Am. Bull.* **86,** 555–70.

Nash, W. P. (1973) Plagioclase resorption phenomena and geobarometry in basic lavas. *Am. Geophys. Union. E.O.S.* **54,** 507.

Roeder, P. L. and Emslie, R. F. (1970) Olivine-liquid equilibrium. *Contrib. Mineral. Petrol.* **29,** 275–89.

Wilkinson, J. F. G. and le Maitre, R. W. (1987) Upper mantle amphiboles and micas and TiO_2, K_2O and P_2O_5 abundances and $100Mg/(Mg+Fe^{2+})$ ratios of common basalts and andesites: implications for modal mantle metasomatism and undepleted mantle compositions. *J. Petrol.* **28,** 37–73.

[*Manuscript received 10 June 1987; revised 15 September 1987*]